



Quantify Oceanic Moisture Contribution to the Tibetan Plateau

Ying Li^{1,2}, Chenghao Wang³, Ru Huang⁴, Denghua Yan⁵, Hui Peng^{1,2}, and Shangbin Xiao^{1,2}

¹Engineering Research Center of Eco-environment in Three Gorges Reservoir Region, Yichang 443002, China;

²College of Hydraulic and Environmental Engineering, China Three Gorges University, Yichang, 443002, China

5 ³Department of Earth System Science, Stanford University, Stanford, CA 94305, USA

⁴Ministry of Emergency Management of China, National Institute of Natural Hazards, Beijing 100085, China

⁵State Key Laboratory of Simulation and Regulation of Water Cycle in River Basin, Water Resources Department, China Institute of Water Resources and Hydropower Research (IWHR), Beijing, 100038, China

Correspondence to: Ying Li (ly_hyrdo@outlook.com); Hui Peng (hpeng1976@163.com)

10 **Abstract.** Evaporation from global oceans is an important moisture source of glaciers and headwaters of major Asia rivers in the Tibetan Plateau (TP). Although recent accelerated global hydrological cycle, altered sea-land thermal contrast, and amplified warming rate over the TP are known to have profound effects on the regional water balance, the contribution of oceanic evaporation, in particular its spatial variability over the vast TP, remains unclear. The lack of such knowledge hinders an accurate quantification of regional water budgets and the reasonable interpretation of water isotope records from
15 observations and paleo archives. Based on historical data and moisture tracking, this study systematically quantifies the absolute and relative contributions of oceanic moisture to the long-term TP precipitation. Results show that seasonal absolute and relative oceanic contributions are generally out of phase, revealing previously overlooked oceanic moisture contributions to the TP in winter as dominated by the westerlies and overestimated moisture contribution from the Indian Ocean in summer. Especially, the relative contribution of moisture from Indian Ocean is only ~30% in the southern TP and further
20 decreases to below 10% in the northern TP. Absolute oceanic contributions explain the dipole pattern of long-term precipitation trends across the southern slope of the Himalayas and the central-northern TP. In comparison, the seasonality of relative oceanic contribution is associated with that of precipitation isotopes across the TP.

1 Introduction

Evaporation from oceans is one of the most important elements in global hydrological cycle, which constitutes more than 80%
25 of the global surface evaporation and contributes to about 60% of terrestrial precipitation (Van der Ent *et al.*, 2010; Trenberth *et al.*, 2011). The global-warming-induced increase of water-holding capacity in the atmosphere, intensification of land-sea thermal gradient, and the relevant moisture limitation over land (i.e., soil moisture limitation) collectively enhance the role of oceanic evaporation in global hydrological cycle (Findell *et al.*, 2019; Algarra *et al.*, 2020; Gimeno *et al.*, 2020b). Regionally, large spatial and temporal variabilities in oceanic evaporation and its contributions to land precipitation exist due to complex
30 circulation systems and energy intensive processes (Gimeno *et al.*, 2013; Van der Ent and Savenije, 2013). Specifically, continental regions influenced by monsoon systems have been considered to benefit more from oceanic evaporation (Gimeno



et al., 2010). One example is the high-elevation Tibetan Plateau (TP)(*Yao et al.*, 2012; *Yao et al.*, 2013; *Yao et al.*, 2018). Although located far from oceans, the TP has long been considered as a gigantic “air pump”, which attracts low-latitude oceanic moisture up to the Asian continent, due to its large-scale topography and thermal forcing(*Xu et al.*, 2014; *Wu et al.*, 2015; *Liu et al.*, 2020). This region sustains freshwater supplies for more than 10 major Asia rivers affecting billions of livelihoods downstream(*Immerzeel et al.*, 2010; *Lutz et al.*, 2014), but is now undergoing dramatic hydrological changes (e.g., the intensive cryosphere melt and lakes expansion)(*Yao et al.*, 2012; *Zhang et al.*, 2020). Meteorological records reveal that the atmospheric warming rate over the TP was twice of the global mean during the past five decades with further accelerations since 1998(*Chen et al.*, 2015; *Duan and Xiao*, 2015; *Kuang and Jiao*, 2016). The consequent changes in the huge land–sea thermal gradient may have significantly altered the regional moisture transport process and circulation systems(*Wang et al.*, 2019).

Hydrological conditions in different parts of the TP are closely connected through the interaction between the mid-latitude westerlies and the Indian Summer Monsoon (ISM) and strong local recycling(*Xu et al.*, 2008; *Yao et al.*, 2013; *Curio and Scherer*, 2016). During monsoon season (June–September), the regional heating significantly enhances the southwesterly monsoon circulations over the northern Indian Ocean, which brings enormous amount of moisture to south Asia and the TP(*Xu et al.*, 2008; *Wu et al.*, 2015). However, the impacts of ISM have gone through changes in recent decades. The rapid Indian Ocean warming during the 20th century potentially weakened the land-sea thermal contrast, leading to the dampening of the summer monsoon Hadley circulation(*Bingyi*, 2005; *Roxy et al.*, 2015). After 2002, the ISM revived due to the increased land-ocean temperature gradient driven by the enhanced warming over the Indian subcontinent and slowed warming over the Indian Ocean(*Jin and Wang*, 2017). All these changes may have altered the oceanic moisture contribution to the TP precipitation. In fact, the hinterland TP (mainly the central-north) is becoming wetter during the recent 50 years, while a drying trend was detected near the southeastern boundary of the TP(*Yang et al.*, 2014; *Jiang and Ting*, 2017; *Wang et al.*, 2018). Some recent studies have quantified the regional average relative contributions of oceanic moisture to the TP precipitation (e.g., 21% in the midwestern TP(*Zhang et al.*, 2017) and 24%–30% in the endorheic TP(*Li et al.*, 2019)), and have suggested that the westerlies can potentially drive oceanic contributions in winter. However, the spatial variation of the oceanic moisture contribution from the Himalayas to the inner TP and their historical changes have not been examined yet.

On the other hand, an accurate quantification of the oceanic evaporation contributions can also benefit the interpretation of water isotopes and paleoclimate archive records (i.e., ice core, tree ring, lake sediments, and stalagmites) gathered in the TP over the past several decades(*Tian et al.*, 2007; *Joswiak et al.*, 2013; *Yao et al.*, 2013; *Zhu et al.*, 2015; *Kumar et al.*, 2021). Water isotopes—the stable isotopic compositions of hydrogen and oxygen—have been widely used to study the climate and water cycle on the TP as well as its paleoclimate history(*Joswiak et al.*, 2013; *Yao et al.*, 2013). Specifically, extensive evidence from precipitation and ice core isotopes since 1990s demonstrates that the onset of the ISM delivers significant oceanic moisture to the TP as far as the south of 34°–35°N(*Tian et al.*, 2007; *Yao et al.*, 2013). However, a quantitative



understanding of the relationship between moisture sources and spatial-temporal variabilities in water isotopes is still absent, largely hampering the interpretation of hydroclimate significance of the isotope records.

The moisture contribution to a target region can be viewed from two aspects: absolute and relative contributions. Although
70 relative contribution can be calculated from the absolute contribution, the distinctions between these two are non-trivial, and
their differences have rarely been explored over the TP (Zhang *et al.*, 2017; Pan *et al.*, 2018; Chen *et al.*, 2019; Qiu *et al.*,
2019). The absolute contribution, which is critical to water balance, is critical to the understanding of hydrological status and
its changes, while the relative contribution is more relevant for tracer-based studies from the consideration of mass balance
during mixing. Based upon historical reanalysis datasets and moisture tracking simulations, this work seeks to systematically
75 quantify the absolute and relative contributions of oceanic moisture to the TP precipitation, and examine the possible
influences of oceanic contribution on precipitation change and water isotope variations.

2 Method and data

2.1 Numerical atmospheric moisture tracking

The Water Accounting Model-2layers (WAM-2layers) is an Eulerian, a posterior moisture tracking model which can track
80 tagged moisture both forward and backward in time to determine the spatial and temporal distributions of moisture
sources (Van der Ent *et al.*, 2010; Van der Ent, 2014). The two vertical layers in the model are set to deal with the wind shear
in the upper air, and in comparison with Lagrangian models (e.g., FLEXible PARTicle (FLEXPART) dispersion model and
the Hybrid SingleParticle Lagrangian Integrated Trajectory (HYSPLIT) model), the Eulerian grids enable the model to excel
in computation speed and to consider moisture budget from precipitation and evaporation separately (Van der Ent *et al.*, 2013;
85 Van der Ent, 2014). The basic principle in WAM-2layers is the atmospheric water balance:

$$\frac{\partial S_k}{\partial t} = \frac{\partial(S_k u)}{\partial x} + \frac{\partial(S_k v)}{\partial y} + E_k - P_k + \xi_k \pm F_V \quad (1)$$

where S_k is the atmospheric moisture storage in layer k ; t is time; u and v are wind speeds in zonal (x) and meridional (y)
directions, respectively; E_k and P_k are evaporation entering layer k and precipitation loss from layer k , respectively; ξ_k is the
residual and F_V is the vertical moisture exchange between the two layers. Note that E_k only applies to bottom layer. The
90 ‘well-mixed’ assumption is applied to this model, which means the precipitation is assumed to be immediately removed from
the atmosphere in the tracking process. Due the existence of residual ξ_k , the closure of the model is defined by a ratio of
residuals between the two layers, i.e., $\xi_{top}/S_{top} = \xi_{bottom}/S_{bottom}$.

In the tracking process, the spatial resolution of Eulerian grid is reduced to $1^\circ \times 1^\circ$, and the time step is set as 0.25 h, to
95 maintain the precision and numerical stability. The vertical separation between the two layers is prescribed as around 812



hPa at the normal atmospheric pressure (Van der Ent *et al.*, 2013). Based on our preliminary tests, we define the tracking domain as from -30°S to 80°N and from -40°W to 140°E , which covers nearly all the potential ocean and land sources.

In a Eulerian grid cell (x, y) in time t , the relative contribution (%) from oceanic evaporation was defined as:

$$100 \quad \rho_o(t, x, y) = \frac{M_o(t, x, y)}{M_o(t, x, y) + M_l(t, x, y)} \quad (2)$$

where M_o and M_l represent the absolute contribution of moisture from oceanic and terrestrial (include local recycling) evaporation, respectively. The ocean and land distributions were defined according to the $1^{\circ} \times 1^{\circ}$ gridded land-sea mask from ERA-Interim.

2.2 Data source

105 Three atmospheric reanalysis products, namely the European Centre for Medium Range Weather Forecasts interim reanalysis dataset (ERA-Interim) (Dee *et al.*, 2011), the National Aeronautics and Space Administration Modern-Era Retrospective Analysis for Research and Applications version 2 dataset (MERRA-2) (Gelaro *et al.*, 2017), and the Japanese
110 55-year Reanalysis dataset (JRA-55) (Kobayashi *et al.*, 2015), are used to drive the WAM-2layers with the following variables: surface pressure (6h), precipitation (3h), evaporation (3h), specific humidity (6h, 17 layers), wind fields (6h, 17
115 layers), total column water (6h), and vertical integrated moisture fluxes (6h). To better represents the water transport in the atmosphere, the moisture in this study represents all possible phases of water in the atmosphere, which contains water vapor, cloud liquid water and cloud frozen water. Note that JRA-55 does not contain the liquid and frozen water fluxes, thus only the water vapor flux is considered. The time span of moisture tracking is 1979–2015 for ERA-Interim and JRA-55, and 1980–2015 for MERRA-2. All variables are temporally resampled to 0.25 h and spatially interpolated to $1^{\circ} \times 1^{\circ}$ grids by
120 bilinear method for consistency.

The $1^{\circ} \times 1^{\circ}$ gridded precipitation dataset adopted in this study during 1979–2015 is the Global Precipitation Climatology Centre (GPCC) dataset, which provides globally gridded gauge-analysis products derived from quality-controlled station observations (Schneider *et al.*, 2018). The event-based precipitation $\delta^{18}\text{O}$ data from 19 observation stations of the Tibetan
120 Network for Isotopes in Precipitation (TNIP) are also used in this work (Yao *et al.*, 2013).

3 Results

3.1 Absolute and relative oceanic moisture contributes to the TP

The absolute and relative contributions (in mm and %, respectively) of global oceanic evaporation to the TP precipitation over the past three decades are tracked forward based on a Eulerian moisture tracking model (WAM-2layers) and three
125 reanalysis products (ERA-Interim, MERRA-2, and JRA-55). The spatial patterns of absolute contribution (Figures 1a–e)



agrees well with the previous understanding that the ISM brings large amount of Indian ocean moisture to the southeastern TP and concentrates around the Brahmaputra Canyon in summer (Xu *et al.*, 2014; Wu *et al.*, 2015). This massive oceanic moisture also stretches westward along the southwest slope of the Himalayas, with a relatively weak westerly moisture sink around the Pamirs mainly in spring and winter, as induced by orographic precipitation (Curio and Scherer, 2016). In summer, the absolute oceanic moisture contribution exhibits a sudden drop from more than 1,000 mm along the southern TP to only about 100 mm in the central-north TP, after climbing the orographic barriers of the Gangdise and the southern slope of Tanggula Mountains.

From the perspective of relative contribution, the oceanic evaporation is responsible for 36%–39% of the total moisture condensation over the TP, and spatially, the relative contribution gradually decreases from more than 50% along the southeastern edge of the TP to less than 20% in the central-northern TP (Figure 1f). Seasonally, the relative contributions of oceanic evaporation to the TP precipitation are 33%–41%, 36%–39%, 35%–38%, and 51%–54% in spring, summer, autumn, and winter, respectively. In spring and autumn, the relative contribution decreases gradually from the southwestern and southern parts to the central-northern TP. In summer, the relative contribution exhibits a roughly zonal distribution, with the 50% isoline located between 25°N and 30°N and the 30% isoline between 30°N and 35°N. This pattern is distinct from that of absolute contribution featured by the oceanic moisture concentrates around the southeast TP. It is also notable that the westernmost TP shows the lowest relative contribution from oceans in summer, which indicates a more active role of the land surface evapotranspiration in the region during the monsoon season.

The largest contrast between absolute and relative contributions occurs in winter: the absolute contribution reaches the lowest level but relative contribution the highest. Based on backward tracking of seasonal precipitation sources of the entire TP, the moisture contribution from the westerlies dominated oceans (the Mediterranean, the Red Sea, the Persian Gulf, and even the Atlantic) is much higher than that from the cold and dry Eurasian continent in winter (Figure S1). The westerlies push the 50% isoline of relative contribution eastward to the mid-eastern TP, with the relative contribution well above 30% for the entire TP. The observed spatial patterns are robust across different simulations, as shown in Figures S2 and S3. Seasonally (Figure 2a), the absolute and relative contributions are in general out of phase and characterized by high relative (absolute) contribution in winter (summer) and low relative (absolute) contribution in summer (winter), despite the enormous Indian moisture transported by the ISM in summer (Figure 2c).

3.2 Oceanic moisture contribution from different oceans

The backward tracking of precipitation of the TP region shows the moisture source could extend far west to the Atlantic as driven by the mid-latitude westerlies and far south to the southern Indian Ocean as dominated by the monsoon system (Figure S4). Given the importance of the westerlies and the ISM in determining TP's climate and hydrologic cycle (Xu *et al.*, 2008; Yao *et al.*, 2013; Curio and Scherer, 2016; Yao *et al.*, 2018), we divide major ocean sources into the western oceans



(WO, contains the Mediterranean, the Red Sea, the Persian Gulf, and the eastern Atlantic) and the Indian Ocean (IO), as
160 shown in Figure S4d.

The absolute contribution of moisture from WO decreases from above 100 mm along the western and southern TP to below
20 mm in the central and northeastern TP (Figure 3a). Seasonally, in addition to most parts of western TP in spring and
winter, the WO also substantially contributes to the precipitation in the southern TP in spring and the southwestern edge of
165 the TP in summer (Figures 3b–e). In comparison, the relative contribution gradually weakens from the northwest to the
southeast of the TP on annual scale (Figure 3f) and in all seasons except summer (Figures 3g, i, and j). This is consistent
with the prevailing orographic precipitation dominated by westerly moisture transport and the zonal movement of the
westerlies (Curio and Scherer, 2016). However, the relative contribution of moisture from WO decreases to below 10% over
the entire TP in summer, because the outbreaking of the ISM and evapotranspiration from the wetting continent dominate the
170 available moisture over the TP (Figures S1a–c). For the intra-annual (monthly) variations of WO moisture contributions to
the entire TP (Figure 2b), the absolute and relative contributions exhibit a phase shift of about three months, with the high
relative (absolute) contribution in spring (winter) and the low relative (absolute) contribution in autumn (summer).

From both absolute and relative perspectives, the moisture contribution from IO (Figure 4) is significantly higher than that
175 from WO, except in the most northwest TP. Consistent with the onset and retreat of the ISM, the absolute contribution from
IO exceeds 500 mm in summer in the southeastern TP and falls to below 100 mm in winter nearly over the entire TP
(Figures 4b–e). The relative contribution from IO exhibits roughly a zonal distribution on annual scale (Figure 4f), with the
30% and 10% isolines located around the south and north TP, respectively. This zonal pattern is consistent from spring to
autumn (Figures 4g–i), which indicates a dynamic balance between IO moisture contribution and total moisture convergence
180 during this period. However, this synchronism is broken in winter with the highest level of relative IO contribution shifting
from the southeastern to the southwestern TP (Figure 4j), and this IO moisture is mainly from the Arabian Sea (Figures S1d–
f). In the westerlies dominated winter, the IO is still the major oceanic source in the southern TP, but the dominating oceanic
source shifts to the WO in the western and northern TP. For the monthly variations of IO moisture contributions to the entire
TP (Figure 2c), the absolute and relative contributions both exhibit summer peaks, however, an opposite pattern is also found
185 in winter when the relative contribution at a high level but the absolute contribution a low level. Simulations based on
MERRA-2 and JRA-55 also suggest similar spatial patterns of moisture contribution from WO and IO (Figures S5–8).

3.3 Absolute contribution of oceanic moisture explains precipitation changes

Regional precipitation is fueled by moisture that is either transported directly from oceans or recycled from lands (Gimeno *et al.*, 2020a). Actually, the spatial pattern of absolute oceanic moisture contribution (especially from the IO), rather than the
190 relative contribution, is highly consistent with precipitation distribution (derived from GPCC (Schneider *et al.*, 2018)) over
the TP region on both annual and seasonal scales (Figure S9). This is consistent with the consensus that the onset and retreat



of the ISM dominate precipitation seasonality over the TP (Xu *et al.*, 2014; Curio *et al.*, 2015; Yao *et al.*, 2018). To quantify the impacts of oceanic moisture contribution changes on the inter-annual variability of TP precipitation, we analyze the time-series correlations between GPCC precipitation and multi-datasets-based oceanic moisture contributions during 1979/1980–
195 2015 (Figure S10). Consistently significant positive correlations ($p < 0.05$) are found only for absolute contributions of moisture from total ocean sources and IO. However, large discrepancies in the time series and trends of annual oceanic contributions exist among different reanalysis products (Figure S11); similar discrepancy has been suggested in previous studies on long-term variations of hydrological cycle over the TP (Wang and Zeng, 2012; Li *et al.*, 2019). This discrepancy is further exemplified by the patterns of relative oceanic contribution trends among different datasets (Figure S12).
200 Nevertheless, consistency in spatial patterns of absolute oceanic contribution trends is observed across different forcing datasets, which is in good agreement with precipitation trends derived from the GPCC during the same period over the TP (Figure 5).

A significant decreasing trend of oceanic moisture contribution is found over much of the southeastern TP in all three
205 simulations (Figures 5a–c), although the simulation based on ERA-Interim yields a relatively smaller region with decreasing signals than based on the other two datasets. These decreasing trends further extend northwestward along the southern slope of the Himalayas and the Pamirs, especially in the simulation based on JRA-55. Meanwhile, the increasing trends of oceanic moisture contribution mainly appear in the central-northern TP. The contrasting spatial pattern of absolute moisture contribution trends matches well with the precipitation change in the TP (Figure 5d). Similar consistency is also observed for
210 absolute moisture contribution from IO (Figure S13). In fact, Jiang and Ting (2017) have found a similar dipole pattern of summer precipitation across the southern slope of Himalayas and the central-north TP, and they attributed this to the interactions between the ISM and the TP. Here we further reveal that this dipole pattern is driven by the changes in oceanic moisture contribution (particularly from IO).

3.4 Relative contribution of oceanic moisture associates with patterns of water isotopes

215 Based on numerous precipitation isotopic observations and ice-core records since the 1990s, previous studies have identified three distinct climate regions/domains in the TP, as determined by the westerlies (northern TP), the ISM (southern TP), and their interactions (Tian *et al.*, 2007; Joswiak *et al.*, 2013; Yao *et al.*, 2013). Theoretically, the moisture delivered by the ISM tends to have relatively low isotope values due to strong convection activities along its transport paths, whereas the moisture delivered by the westerlies in general has relatively high isotope values (Bowen *et al.*, 2019; Cai and Tian, 2020). Here we
220 further investigate the relationships between the quantified oceanic moisture contributions and precipitation $\delta^{18}\text{O}$ observations at 19 monitoring stations over the TP (Figure 6 and Figures S14–17).

The strongest relationship is found between precipitation $\delta^{18}\text{O}$ and relative oceanic moisture contribution from IO (Figure 6). In the monsoon domain, the $\delta^{18}\text{O}$ is high in spring and low in summer (note the revised $\delta^{18}\text{O}$ axes), and correspondingly,



225 relative contribution from IO is low in spring and high in summer. In comparison, in the westerlies domain, high $\delta^{18}\text{O}$ values
are associated with low relative contributions from IO during the monsoon season, whereas low $\delta^{18}\text{O}$ values are associated
with high relative contributions from IO during other non-monsoon seasons. In the transition domain, the seasonal cycle of
 $\delta^{18}\text{O}$ and relative contribution from IO are in an intermediate state. Note the mismatches between summer peaks of relative
moisture from IO and low $\delta^{18}\text{O}$ values in autumn at Lulang, Nuxia, and Bomi near the Brahmaputra Canyon, which is likely
230 attributable to the impact of moisture transported from southeast Asia or the Pacific Ocean driven by the trough embedded in
the southern branch of the westerlies (Cai and Tian, 2020).

Except for several sites in the southmost TP, our result confirms the theory that a higher percentage of oceanic moisture
contribution from the ISM-dominated IO indicates a lower precipitation $\delta^{18}\text{O}$ value over the TP. As for the relative
235 contribution from westerlies dominated WO (Figure S15) and the absolute contributions from both WO (Figure S16) and IO
(Figure S17), their relationships with water isotope ratios are much weak. Based on the seasonality of water isotope ratios,
previous studies have also identified a northmost boundary of the ISM's impact around 34° – 35°N over the TP, where the
Tanggula mountains represent the main orographic barrier (Tian *et al.*, 2007; Joswiak *et al.*, 2013; Yao *et al.*, 2013).
Quantitatively, this geographical barrier of the monsoon system reflected in water isotope ratios is closely aligned with the
240 10%–20% isoline of the relative contribution from IO and 20%–30% isoline of the absolute oceanic moisture contribution in
summer.

5 Conclusions and discussion

From the perspectives of absolute and relative contributions, this work quantifies the oceanic evaporation contributions to
precipitation over the TP region. After crossing the surrounding mountain ranges of the TP, the absolute (relative)
245 contribution of moisture from global oceans rapidly decreases from more than 1000 mm (50%) around the Brahmaputra
Canyon to only about 100 mm (10%) in the central-northern TP. However, substantial variations in the spatial patterns exist
at the seasonal scale. For example, the highest absolute contribution of oceanic evaporation to the TP occurs in the southeast
in summer, while the highest relative contribution occurs in the western TP in winter. Specifically, previous studies primarily
focused on oceanic moisture contributions to the TP precipitation from the monsoon-dominated Indian Ocean (Xu *et al.*, 2008;
250 Yao *et al.*, 2013). In contrast, our results highlight that the westerlies-dominated oceans, such as the Mediterranean, the Red
Sea, the Persian Gulf, and even the Atlantic, are also important sources of the TP precipitation, especially during the non-
monsoon seasons.

In addition, we found that the absolute contribution of oceanic moisture is more consistent with precipitation patterns, while
255 the relative contribution to some extent reflects the variations of precipitation isotopes. Especially, the spatial pattern of
trends in absolute oceanic moisture contributions (particularly from IO) explains the dipole pattern of precipitation change



across the southern slope of the Himalayas and the central-northern TP. Meanwhile, the seasonal variations of relative contribution from IO are generally out of phase with precipitation $\delta^{18}\text{O}$ over much of the TP in different climate domains. We acknowledge that beyond the influence from moisture sources, precipitation is also jointly affected by multiple synoptic and climate factors and so are the precipitation isotopes (Dansgaard, 1964; Galewsky *et al.*, 2016; Bowen *et al.*, 2019). Nevertheless, this work systematically quantifies the oceanic moisture contributes to the vast TP, and provides new insights into the influence of oceanic moisture contribution on water cycle and water isotope records in the region. Future studies on multi-source moisture transport are expected to further enrich our understanding of paleoclimate proxy records and global warming induced water resource change over the TP—the “Asia water tower” and the core area of the Belt and Road Initiative.

Data availability

The ERA-Interim dataset can be downloaded from the official website of the European Centre for Medium-Range Weather Forecasts (ECMWF; <https://www.ecmwf.int/en/forecasts/datasets/reanalysis-datasets/era-interim>). The MERRA-2 dataset is available from <https://gmao.gsfc.nasa.gov/reanalysis/MERRA-2/>, which is managed by the Goddard Earth Sciences Data and Information Services Center (GES DISC), National Aeronautics and Space Administration (NASA). The JRA-55 product was developed by the Japan Meteorological Agency and can be downloaded from <https://jra.kishou.go.jp/>. The GPCC precipitation dataset is operated by Deutscher Wetterdienst (DWD) under the auspices of the World Meteorological Organization (WMO), and can be downloaded from <https://www.dwd.de/EN/ourservices/gpcc/gpcc.html>. The TNIP $\delta^{18}\text{O}$ data is provided by the National Tibetan Plateau Data Center (<http://data.tpdc.ac.cn>).

Author contribution

YL and CW conceptualized the study. YL carried out numerical simulations, conducted formal analysis, and prepared figures, and wrote the initial draft. YL, CW, and RH contributed to the visualization of results. All authors contributed to the review and editing of the manuscript.

Competing interests

The authors declare that they have no conflict of interest.



Acknowledgements

This work was financially supported by the Second Tibetan Plateau Scientific Expedition and Research Program (2019QZKK020705). We thank Dr. Zhongyin Cai for his revision of the manuscript, and rewrite the core part of the isotope analysis.

285 References

- Algarra, I., Nieto, R., Ramos, A. M., Eiras-Barca, J., Trigo, R. M., and Gimeno, L.: Significant increase of global anomalous moisture uptake feeding landfalling Atmospheric Rivers, *Nat. Commun.*, 11(1), 5082, <https://doi.org/10.1038/s41467-020-18876-w>, 2020.
- 290 Bingyi, W.: Weakening of Indian summer monsoon in recent decades, *Adv. Atmos. Sci.*, 22(1), 21-29, <https://doi.org/10.1007/BF02930866>, 2005.
- Bowen, G. J., Cai, Z., Fiorella, R. P., and Putman, A. L.: Isotopes in the Water Cycle: Regional- to Global-Scale Patterns and Applications, *Annu. Rev. Earth Planet. Sci.*, 47, 453-479, <https://doi.org/10.1146/annurev-earth-053018-060220>, 2019.
- Cai, Z., and Tian, L.: What Causes the Postmonsoon 18O Depletion Over Bay of Bengal Head and Beyond?, *Geophys. Res. Lett.*, 47(4), e2020GL086985, <https://doi.org/10.1029/2020GL086985>, 2020.
- 295 Chen, B., Zhang, W., Yang, S., and Xu, X. D.: Identifying and contrasting the sources of the water vapor reaching the subregions of the Tibetan Plateau during the wet season, *Climate Dyn.*, 53(11), 6891-6907, <https://doi.org/10.1007/s00382-019-04963-2>, 2019.
- Chen, D., Xu, B., Yao, T., Guo, Z., Cui, P., Chen, F., Zhang, R., ZHANG, X., ZHANG, Y., and FAN, J.: Assessment of past, present and future environmental changes on the Tibetan Plateau, *Chin. Sci. Bull.*, 60(32), 3025-3035, <https://doi.org/10.1360/N972014-01370>, 2015.
- 300 Curio, J., Maussion, F., and Scherer, D.: A 12-year high-resolution climatology of atmospheric water transport over the Tibetan Plateau, *Earth Syst. Dynam.*, 6(1), 109-124, <https://doi.org/10.5194/esd-6-109-2015>, 2015.
- Curio, J., and Scherer, D.: Seasonality and spatial variability of dynamic precipitation controls on the Tibetan Plateau, *Earth Syst. Dynam.*, 7(3), 767-782, <https://doi.org/10.5194/esd-7-767-2016>, 2016.
- 305 Dansgaard, W.: Stable isotopes in precipitation, *Tellus*, 16(4), 436-468, <https://doi.org/10.3402/tellusa.v16i4.8993>, 1964.
- Dee, D., Uppala, S., Simmons, A., Berrisford, P., Poli, P., Kobayashi, S., Andrae, U., Balmaseda, M., Balsamo, G., and Bauer, P.: The ERA-Interim reanalysis: Configuration and performance of the data assimilation system, *Quart. J. Roy. Meteorol. Soc.*, 137(656), 553-597, <https://doi.org/10.1002/qj.828>, 2011.
- Duan, A., and Xiao, Z.: Does the climate warming hiatus exist over the Tibetan Plateau?, *Sci Rep*, 5, 13711, <https://doi.org/10.1038/srep13711>, 2015.
- 310 Findell, K. L., Keys, P. W., van der Ent, R. J., Lintner, B. R., Berg, A., and Krasting, J. P.: Rising Temperatures Increase Importance of Oceanic Evaporation as a Source for Continental Precipitation, *J. Climate*, 32(22), 7713-7726, <https://doi.org/10.1175/jcli-d-19-0145.1>, 2019.
- Galewsky, J., Steen-Larsen, H. C., Field, R. D., Worden, J., Risi, C., and Schneider, M.: Stable isotopes in atmospheric water vapor and applications to the hydrologic cycle, *Rev. Geophys.*, 54(4), 809-865, <https://doi.org/10.1002/2015rg000512>, 2016.
- 315 Gelaro, R., McCarty, W., Suárez, M. J., Todling, R., Molod, A., Takacs, L., Randles, C. A., Darmenov, A., Bosilovich, M. G., and Reichle, R.: The modern-era retrospective analysis for research and applications, version 2 (MERRA-2), *J. Climate*, 30(14), 5419-5454, <https://doi.org/10.1175/JCLI-D-16-0758.1>, 2017.
- 320 Gimeno, L., Drumond, A., Nieto, R., Trigo, R. M., and Stohl, A.: On the origin of continental precipitation, *Geophys. Res. Lett.*, 37(13), 153-188, <https://doi.org/10.1029/2010GL043712>, 2010.
- Gimeno, L., Nieto, R., Drumond, A., Castillo, R., and Trigo, R.: Influence of the intensification of the major oceanic moisture sources on continental precipitation, *Geophys. Res. Lett.*, 40(7), 1443-1450, <https://doi.org/10.1002/grl.50338>, 2013.



- 325 Gimeno, L., Nieto, R., and Sori, R.: The growing importance of oceanic moisture sources for continental precipitation, *Npj Climate and Atmospheric Science*, 3(1), 27, <https://doi.org/10.1038/s41612-020-00133-y>, 2020a.
- Gimeno, L., Vazquez, M., Eiras-Barca, J., Sori, R., Stojanovic, M., Algarra, I., Nieto, R., Ramos, A. M., Duran-Quesada, A. M., and Dominguez, F.: Recent progress on the sources of continental precipitation as revealed by moisture transport analysis, *Earth-Sci. Rev.*, 201, 103070, <https://doi.org/10.1016/j.earscirev.2019.103070>, 2020b.
- 330 Immerzeel, W. W., Van Beek, L. P., and Bierkens, M. F.: Climate change will affect the Asian water towers, *Science*, 328(5984), 1382-1385, <https://doi.org/10.1126/science.1183188> 2010.
- Jiang, X. W., and Ting, M. F.: A Dipole Pattern of Summertime Rainfall across the Indian Subcontinent and the Tibetan Plateau, *J. Climate*, 30(23), 9607-9620, <https://doi.org/10.1175/Jcli-D-16-0914.1>, 2017.
- Jin, Q., and Wang, C.: A revival of Indian summer monsoon rainfall since 2002, *Nat. Climate Chang.*, 7(8), 587-595, <https://doi.org/10.1038/NCLIMATE3348>, 2017.
- 335 Joswiak, D. R., Yao, T., Wu, G., Tian, L., and Xu, B.: Ice-core evidence of westerly and monsoon moisture contributions in the central Tibetan Plateau, *J. Glaciol.*, 59(213), 56-66, <https://doi.org/10.3189/2013JogG12J035> 2013.
- Kobayashi, S., Ota, Y., Harada, Y., Ebata, A., Moriya, M., Onoda, H., Onogi, K., Kamahori, H., Kobayashi, C., and Endo, H.: The JRA-55 reanalysis: General specifications and basic characteristics, *J. Meteor. Soc. Japan*, 93(1), 5-48, <https://doi.org/10.2151/jmsj.2015-001>, 2015.
- 340 Kuang, X., and Jiao, J. J.: Review on climate change on the Tibetan Plateau during the last half century, *J. Geophys. Res.-Atmos.*, 121, 3979-4007, <https://doi.org/10.1002/2015JD024728>, 2016.
- Kumar, O., Ramanathan, A. L., Bakke, J., Kotlia, B. S., Shrivastava, J. P., Kumar, P., Sharma, R., and Kumar, P.: Role of Indian Summer Monsoon and Westerlies on glacier variability in the Himalaya and East Africa during Late Quaternary: Review and new data, *Earth-Sci. Rev.*, 212, 103431, <https://doi.org/10.1016/j.earscirev.2020.103431>, 2021.
- 345 Li, Y., Su, F., Chen, D., and Tang, Q.: Atmospheric Water Transport to the Endorheic Tibetan Plateau and Its Effect on the Hydrological Status in the Region, *J. Geophys. Res.-Atmos.*, 124(23), 12864-12881, <https://doi.org/10.1029/2019jd031297>, 2019.
- Liu, Y., Lu, M., Yang, H., Duan, A., He, B., Yang, S., and Wu, G.: Land-atmosphere-ocean coupling associated with the Tibetan Plateau and its climate impacts, *Natl. Sci. Rev.*, 7(03), 534-552, <https://doi.org/10.1093/nsr/nwaa011>, 2020.
- Lutz, A. F., Immerzeel, W. W., Shrestha, A. B., and Bierkens, M. F. P.: Consistent increase in High Asia's runoff due to increasing glacier melt and precipitation, *Nat. Climate Chang.*, 4(7), 587-592, <https://doi.org/10.1038/nclimate2237>, 2014.
- 355 Pan, C., Zhu, B., Gao, J., Kang, H., and Zhu, T.: Quantitative identification of moisture sources over the Tibetan Plateau and the relationship between thermal forcing and moisture transport, *Climate Dyn.*, 52(1-2), 181-196, <https://doi.org/10.1007/s00382-018-4130-6>, 2018.
- Qiu, T., Huang, W., Wright, J. S., Lin, Y., Lu, P., He, X., Yang, Z., Dong, W., Lu, H., and Wang, B.: Moisture Sources for Wintertime Intense Precipitation Events Over the Three Snowy Subregions of the Tibetan Plateau, *J. Geophys. Res.-Atmos.*, 124(23), 12708-12725, <https://doi.org/10.1029/2019jd031110>, 2019.
- 360 Roxy, M. K., Ritika, K., Terray, P., Murtugudde, R., Ashok, K., and Goswami, B. N.: Drying of Indian subcontinent by rapid Indian Ocean warming and a weakening land-sea thermal gradient, *Nat Commun*, 6, 7423, <https://doi.org/10.1038/ncomms8423>, 2015.
- Schneider, U., Becker, A., Finger, P., Meyer-Christoffer, A., and Ziese, M.: GPCC Full Data Monthly Product Version 2018 at 1.0°: Monthly Land-Surface Precipitation from Rain-Gauges built on GTS-based and Historical Data, Global Precipitation Climatology Centre (GPCC), https://doi.org/10.5676/DWD_GPCC/FD_M_V2018_100, 2018.
- 365 Tian, L., Yao, T., MacClune, K., White, J., Schilla, A., Vaughn, B., Vachon, R., and Ichiyonagi, K.: Stable isotopic variations in west China: a consideration of moisture sources, *Journal of Geophysical Research: Atmospheres* (1984–2012), 112(D10), D10112, <https://doi.org/10.1029/2006JD007718>, 2007.
- Trenberth, K. E., Fasullo, J. T., and Mackaro, J.: Atmospheric Moisture Transports from Ocean to Land and Global Energy Flows in Reanalyses, *J. Climate*, 24(18), 4907-4924, <https://doi.org/10.1175/2011JCLI4171.1>, 2011.
- 370 Van der Ent, R. J.: A new view on the hydrological cycle over continents., Delft University of Technology, Netherlands, Ph.D., 96 pp., doi:10.4233/uuid:0ab824ee-6956-4cc3-b530-3245ab4f32be, 2014.
- Van der Ent, R. J., and Savenije, H. H.: Oceanic sources of continental precipitation and the correlation with sea surface temperature, *Water Resour. Res.*, 49(7), 3993-4004, <https://doi.org/10.1002/wrcr.20296>, 2013.



- 375 Van der Ent, R. J., Savenije, H. H., Schaefli, B., and Steele-Dunne, S. C.: Origin and fate of atmospheric moisture over continents, *Water Resour. Res.*, 46(9), W09525, <https://doi.org/10.1029/2010WR009127>, 2010.
- Van der Ent, R. J., Tuinenburg, O. A., Knoche, H. R., Kunstmann, H., and Savenije, H. H. G.: Should we use a simple or complex model for moisture recycling and atmospheric moisture tracking?, *Hydrol. Earth Syst. Sci.*, 17(12), 4869-4884, <https://doi.org/10.5194/hess-17-4869-2013>, 2013.
- 380 Wang, A., and Zeng, X.: Evaluation of multireanalysis products with in situ observations over the Tibetan Plateau, *J. Geophys. Res.-Atmos.*, 117(D5), D05102, <https://doi.org/10.1029/2011JD016553>, 2012.
- Wang, X., Pang, G., and Yang, M.: Precipitation over the Tibetan Plateau during recent decades: a review based on observations and simulations, *Int. J. Climatol.*, 38(3), 1116-1131, <https://doi.org/10.1002/joc.5246> 2018.
- Wang, Z., Duan, A., and Yang, S.: Potential regulation on the climatic effect of Tibetan Plateau heating by tropical air-sea coupling in regional models, *Climate Dyn.*, 52(3), 1685-1694, <https://doi.org/10.1007/s00382-018-4218-z>, 2019.
- 385 Wu, G., Duan, A., Liu, Y., Mao, J., Ren, R., Bao, Q., He, B., Liu, B., and Hu, W.: Tibetan Plateau climate dynamics: recent research progress and outlook, *Natl. Sci. Rev.*, 2(1), 100-116, <https://doi.org/10.1093/nsr/nwu045> 2015.
- Xu, X., Lu, C., Shi, X., and Gao, S.: World water tower: An atmospheric perspective, *Geophys. Res. Lett.*, 35(20), L20815, <https://doi.org/10.1029/2008gl035867>, 2008.
- 390 Xu, X., Zhao, T., Lu, C., Guo, Y., Chen, B., Liu, R., Li, Y., and Shi, X.: An important mechanism sustaining the atmospheric "water tower" over the Tibetan Plateau, *Atmos. Chem. Phys.*, 14(20), 11287-11295, <https://doi.org/10.5194/acp-14-11287-2014>, 2014.
- Yang, K., Wu, H., Qin, J., Lin, C., Tang, W., and Chen, Y.: Recent climate changes over the Tibetan Plateau and their impacts on energy and water cycle: A review, *Glob. Planet. Change*, 112, 79-91, <https://doi.org/10.1016/j.gloplacha.2013.12.001>, 2014.
- 395 Yao, T., Masson-Delmotte, V., Gao, J., Yu, W., Yang, X., Risi, C., Sturm, C., Werner, M., Zhao, H., and He, Y.: A review of climatic controls on $\delta^{18}O$ in precipitation over the Tibetan Plateau: Observations and simulations, *Rev. Geophys.*, 51(4), 525-548, <https://doi.org/10.1002/rog.20023>, 2013.
- Yao, T., Thompson, L., Yang, W., Yu, W. S., Gao, Y., Guo, X. J., Yang, X. X., Duan, K. Q., Zhao, H. B., Xu, B. Q., Pu, J. C., Lu, A. X., Xiang, Y., Kattel, D. B., and Joswiak, D.: Different glacier status with atmospheric circulations in Tibetan Plateau and surroundings, *Nat. Climate Chang.*, 2(9), 663-667, <https://doi.org/10.1038/Nclimate1580>, 2012.
- 400 Yao, T., Xue, Y., Chen, D., Chen, F., Thompson, L., Cui, P., Koike, T., Lau, W. K.-M., Lettenmaier, D., and Mosbrugger, V.: Recent Third Pole's rapid warming accompanies cryospheric melt and water cycle intensification and interactions between monsoon and environment: multi-disciplinary approach with observation, modeling and analysis, *Bull. Amer. Meteorol. Soc.*, 100(3), 423-444, <https://doi.org/10.1175/BAMS-D-17-0057.1> 2018.
- 405 Zhang, C., Tang, Q., and Chen, D.: Recent changes in the moisture source of precipitation over the Tibetan Plateau, *J. Climate*, 30(5), 1807-1819, <https://doi.org/10.1175/JCLI-D-15-0842.1>, 2017.
- Zhang, G., Yao, T., Xie, H., Yang, K., Zhu, L., Shum, C. K., Bolch, T., Yi, S., Allen, S., Jiang, L., Chen, W., and Ke, C.: Response of Tibetan Plateau lakes to climate change: Trends, patterns, and mechanisms, *Earth-Sci. Rev.*, 208, 103269, <https://doi.org/10.1016/j.earscirev.2020.103269>, 2020.
- 410 Zhu, L., Lü, X., Wang, J., Peng, P., Kasper, T., Daut, G., Haberzettl, T., Frenzel, P., Li, Q., Yang, R., Schwalb, A., and Mäusbacher, R.: Climate change on the Tibetan Plateau in response to shifting atmospheric circulation since the LGM, *Sci Rep*, 5(1), 13318, <https://doi.org/10.1038/srep13318>, 2015.

415



Figures

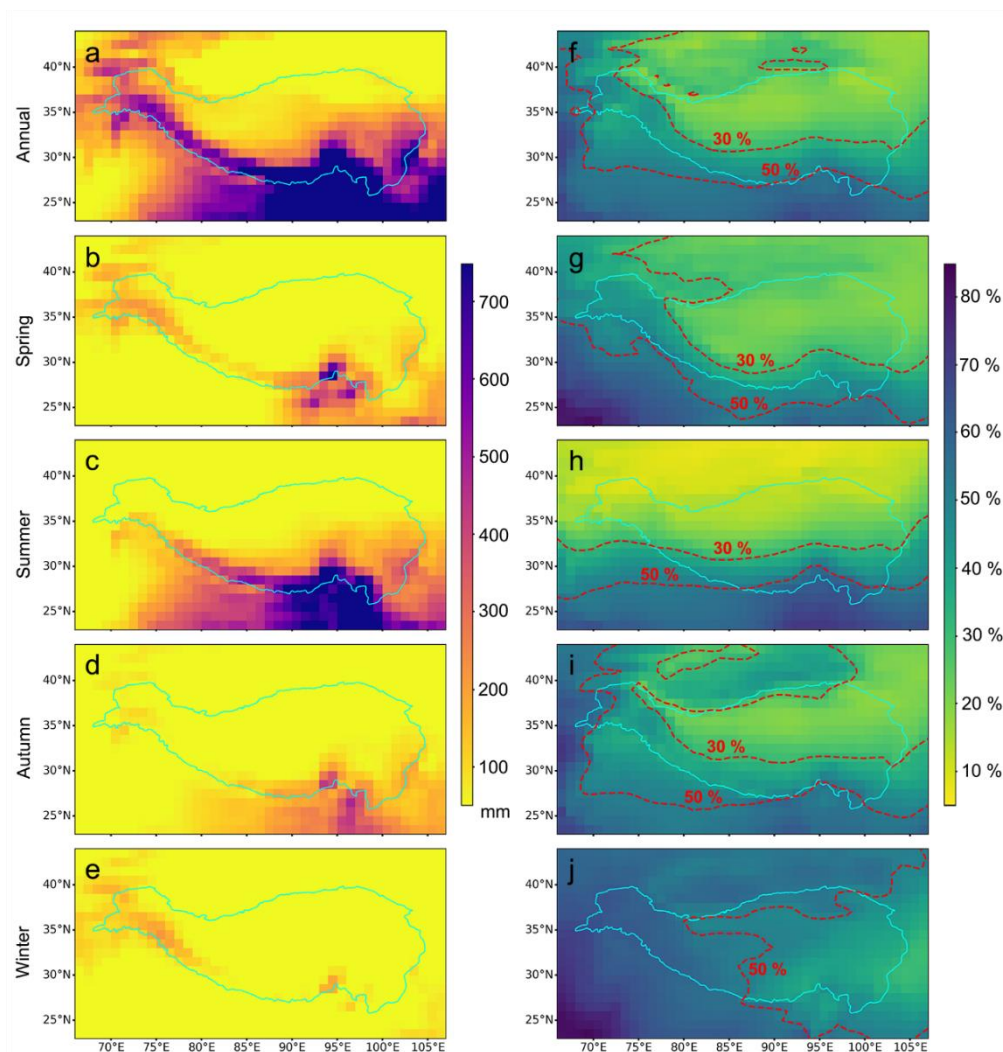


Figure 1: Spatial distributions of long-term mean absolute and relative oceanic moisture contributions to TP precipitation. (a–e) The absolute contribution from global oceans to the TP region (mm, equivalent water height) on annual and seasonal scales. (f–j) The relative contribution of oceanic moisture to the TP region (% , the percentage of oceanic contribution relative to total moisture convergence) on annual and seasonal scales. Cyan lines represent the TP boundary, and dashed red lines in (f–j) are 30% and 50% isolines of relative contribution. The forward moisture tracking results on global oceans are modeled by WAM-2layers forced with ERA-Interim average over 1979–2015. Moisture-tracking results driven by MERRA-2 (1980–2015) and JRA-55 (1979–2015) are shown in Figures S2 and S3, respectively.

425

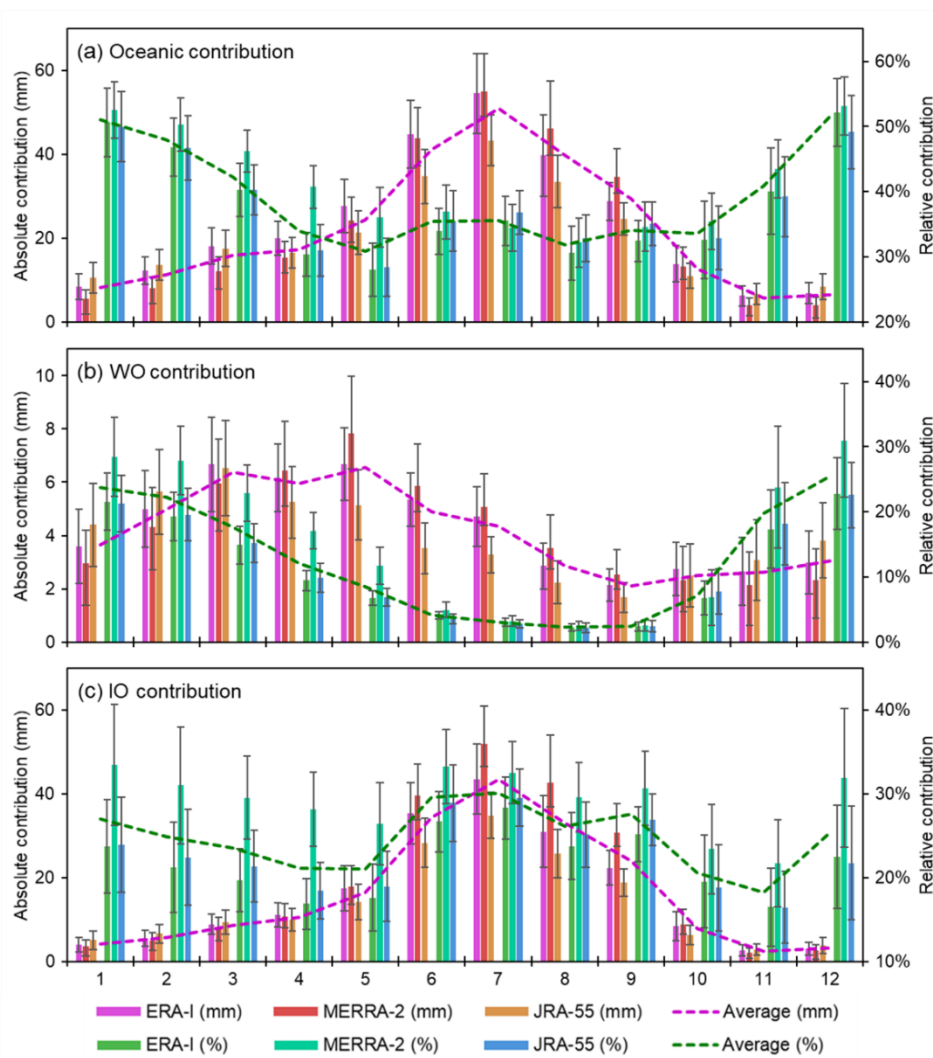
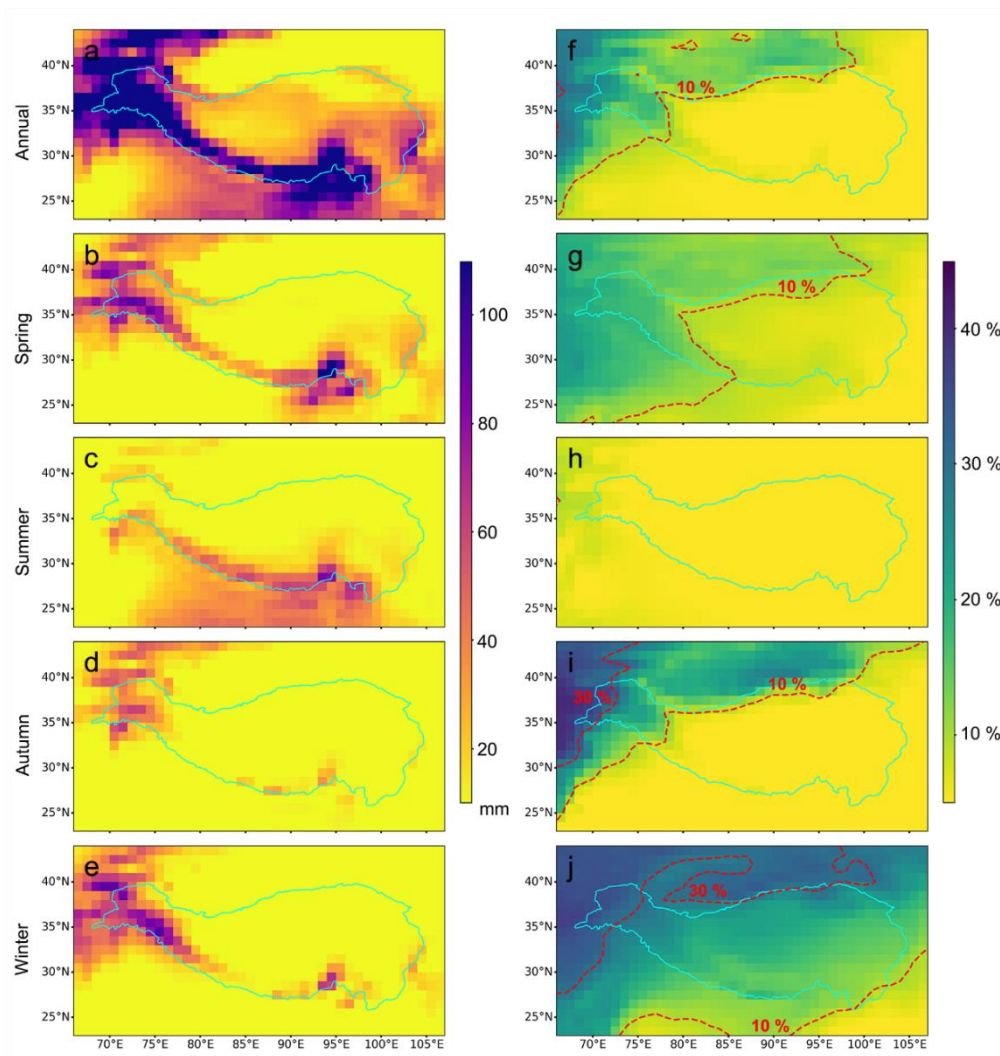
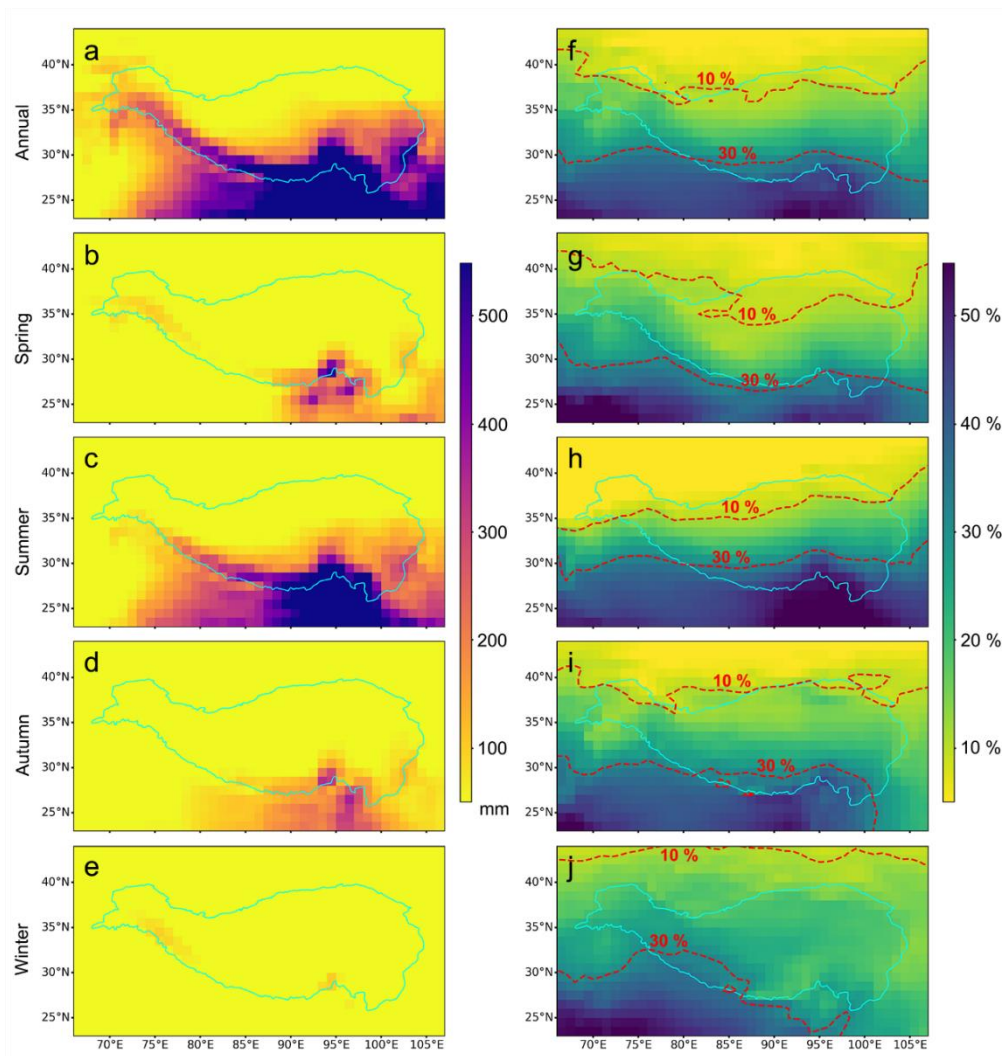


Figure 2: Intra-annual variations of long-term mean absolute and relative oceanic moisture contributions to TP precipitation. a, b, and c represent the oceanic moisture contributes to the TP region from global oceans, WO, and IO, respectively. Pink, red, and yellow bars are absolute contributions (mm); green, cyan, and blue bars are relative contributions (%); all oceanic contributions are simulated by ERA-Interim (1979–2015), MERRA-2 (1980–2015), and JRA-55 (1979–2015). Dashed pink and blue lines in (a-c) are three-datasets-average absolute and relative contributions, respectively. Error bars represent one standard deviation of the interannual variations.



435 **Figure 3:** Spatial distribution of absolute and relative moisture contribution from western oceans (WO) to TP precipitation. (a–e) The absolute contribution from WO to the TP region (mm) on annual and seasonal scales. (f–j) The relative contribution of WO moisture to the TP region (%) on annual and seasonal scales. The dashed red lines in (f–j) are 10% and 30% isolines of relative contribution. The forward moisture tracking results on WO are modeled by WAM-2layers forced with ERA-Interim averaged over 1979–2015. Moisture-tracking results driven by MERRA-2 (1980–2015) and JRA-55 (1979–2015) are shown in Figures S5 and S6, respectively.



440

Figure 4: Spatial distribution of absolute and relative moisture contribution from Indian Ocean (IO) to TP precipitation. (a–e) The absolute contribution from IO to the TP region (mm) on annual and seasonal scales. (f–j) The relative contribution of IO moisture to the TP region (%) on annual and seasonal scales. The dashed red lines in (f–j) are 10% and 30% isolines of relative contribution. The forward moisture tracking results on IO are modeled by WAM-2layers forced with ERA-Interim averaged over 1979–2015. Moisture-tracking results driven by MERRA-2 (1980–2015) and JRA-55 (1979–2015) are shown in Figures S7 and S8, respectively.

445

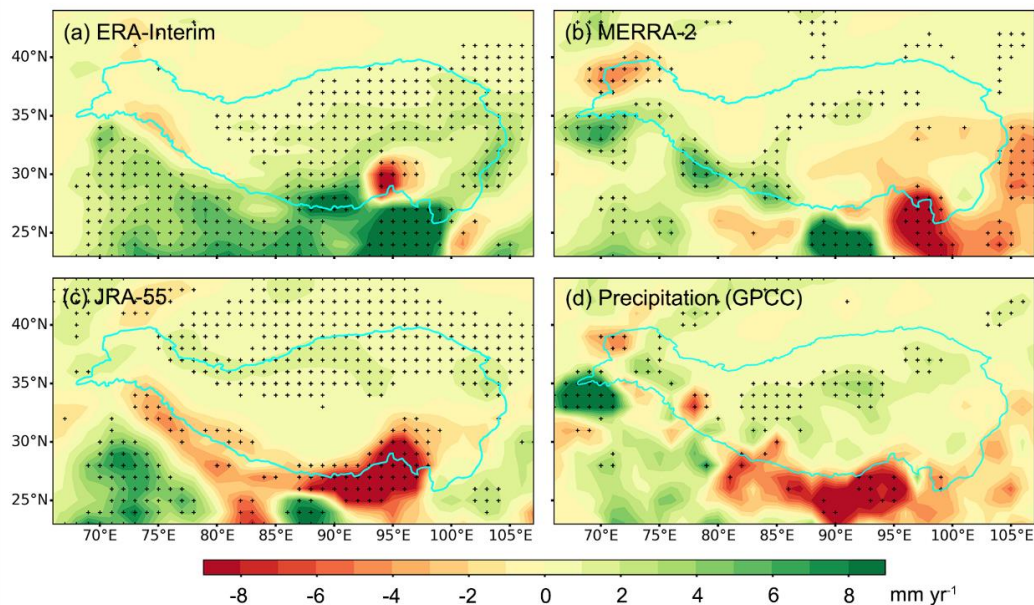


Figure 5: Trends of absolute oceanic moisture contribution and precipitation in the TP region. (a–c) Long-term trends of annual absolute oceanic moisture contribution (mm yr^{-1}) from forward moisture tracking (WAM-2layers) driven by ERA-Interim (1979–2015), MERRA-2 (1980–2015), and JRA-55 (1979–2015), respectively. (d) Long-term trend of annual precipitation derived from GPCC (1979–2015) in the TP region. Stippling indicates regions with statistically significant trends ($p < 0.05$).

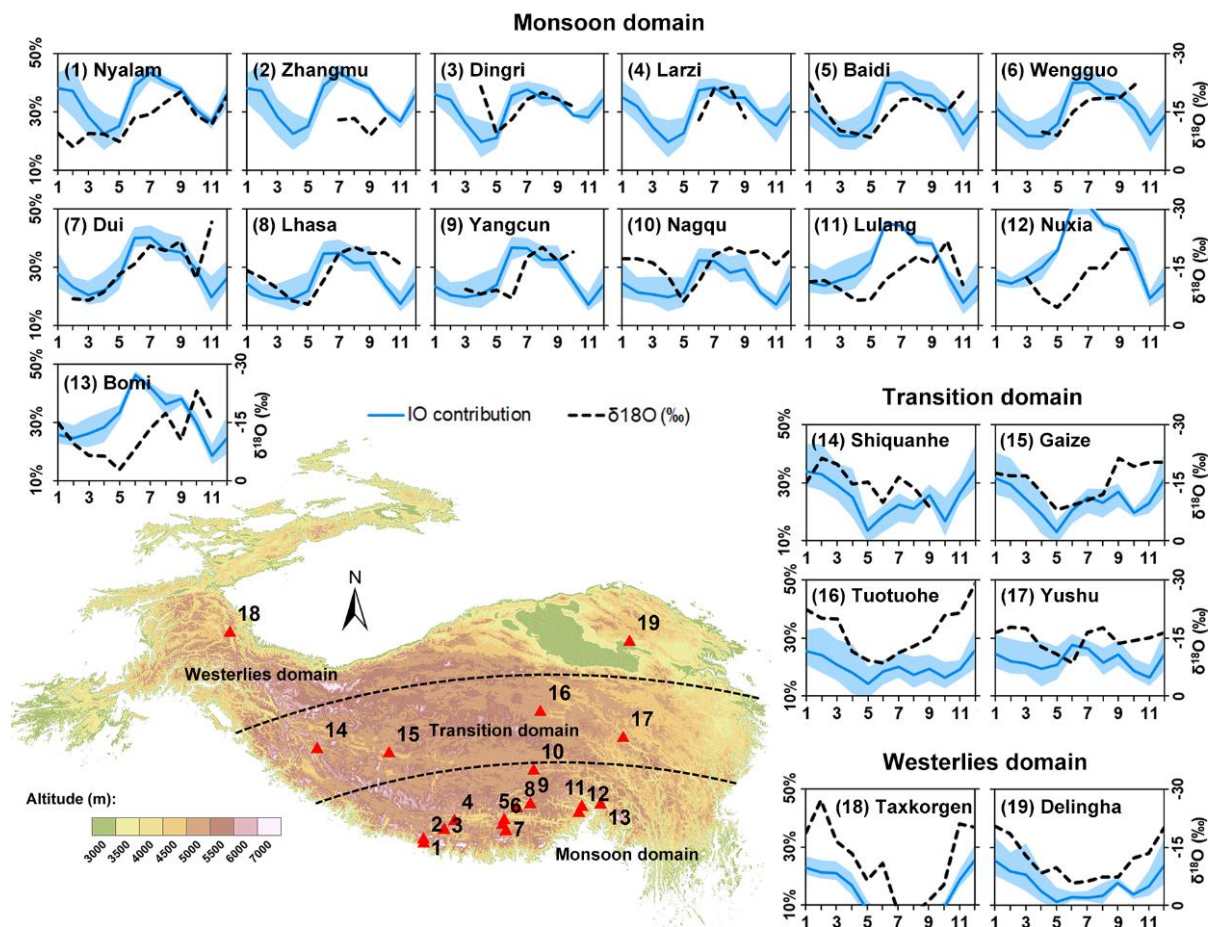


Figure 6: Locations of precipitation isotope monitoring stations and the relationship between monthly relative contributions of moisture from IO (blue lines) and precipitation isotope observations (dotted lines). Sites 1–13, 14–17, and 18–19 represent stations located within the monsoon domain, transition domain, and westerlies domain, respectively. Blue lines show the mean IO moisture contributions based on three simulations, while the shadings show the range (detailed seasonal variations of three simulations are shown in Figure S14). Note that for consistency, oceanic contributions below 10% and above 50% are not shown for sites 12 and 18.